JOURNAL OF CATALYSIS **170,** 20–28 (1997)
ARTICLE NO. CA971728

The Effect of Phosphorus on Oxidic NiMo(CoMo)/γ-Al_2O_3 Catalysts: A Solid State NMR Investigation

H. Kraus and R. Prins

Laboratory for Technical Chemistry, Swiss Federal Institute of Technology (ETH), 8092 Zurich, Switzerland

Received January 27, 1997; revised April 1, 1997; accepted April 11, 1997

The effect of various impregnation procedures on the structures of oxidic phosphorus-containing NiMo/Al_2O_3 and CoMo/Al_2O_3 catalysts was studied by quantitative ^{31}P and ^{27}Al solid state NMR. $NH_4H_2PO_4$ was used as the phosphorus source, since it reacts less strongly with the alumina support than does H_3PO_4. The presence of paramagnetic Co and Ni ions induces strong line broadening and a signal loss in the ^{31}P and ^{27}Al NMR spectra which can be used to deduce the distribution of Co and Ni over the catalyst surface. Large differences in this distribution existed, depending on the paramagnetic ion and the impregnation procedure. The addition of phosphorus led mainly to the formation of Co–Mo–P compounds in samples containing cobalt, whereas the creation of an aluminum phosphate phase was favored in nickel-containing catalysts. An impregnation procedure in which Ni or Co and phosphorus are separately deposited on the catalyst surface also promoted $AlPO_4$ formation, so that even in the samples containing cobalt some aluminum phosphate is observed. On the other hand, coimpregnation of Co or Ni and phosphorus resulted in catalysts which contained little aluminum phosphate. Possible consequences for hydrotreating reactions are discussed.

INTRODUCTION

Catalysts consisting of molybdenum sulfide supported on alumina and promoted by cobalt or nickel are extensively used in the oil processing industry to catalyze hydrotreating reactions such as hydrodesulfurization and hydrodenitrogenation. In the preparation of these catalysts, γ-Al_2O_3 is impregnated with ammonium heptamolybdate and nickel (cobalt) nitrate to obtain an oxidic catalyst precursor which is sulfided afterward. Phosphorus, present as phosphate in the oxidic catalysts, is frequently applied as a modifier element and has been shown to result in an increased hydrodenitrogenation activity (1–4). Various explanations have been given for this improvement. It has been reported that phosphorus enhances the solubility of molybdate by the formation of phosphomolybdate complexes which makes catalyst preparation easier (5–8) and may lead to a different dispersion of the Mo and Co/Ni. Often an increase in molybdenum fractions in easily reducible and sulfidable forms, such as multilayered molybdate, crystalline $Al_2(MoO_4)_3$ and MoO_3, has been observed (9–11). On the other hand, cobalt and nickel are less easily sulfided on phosphorus-containing samples due to an interaction between these metal atoms and an aluminum phosphate phase formed at the support surface (12).

Because Co and Ni ions are paramagnetic, solid state NMR has seldom been used for the study of hydrotreating catalysts. DeCanio *et al.* (10) reported a reduction of signal intensity and relaxation delays in ^{31}P and ^{27}Al NMR investigations of NiP/γ-Al_2O_3 samples. They were able to prove the formation of monomeric and polymeric phosphates as well as $AlPO_4$, similar to results found for P/γ-Al_2O_3 catalysts. A commercial NiMoP/γ-Al_2O_3 catalyst was studied by Haller and co-workers (13–15) with ^{27}Al, ^{31}P, and ^{95}Mo NMR. They observed the formation of crystalline $AlPO_4$ and $Al_2(MoO_4)_3$ after a severe calcination treatment. ^{95}Mo solid state NMR was applied by Edwards and Ellis to CoMo/γ-Al_2O_3 systems; Co was found to induce line broadening, especially in sequentially impregnated catalysts (16).

Reduction of signal intensity and line broadening induced by paramagnetic interactions may, on the other hand, be used to advantage. They allow to estimate how close various compounds are to Co or Ni and thus give information about the distribution of these compounds. In the present study, CoMoP/γ-Al_2O_3 and NiMoP/γ-Al_2O_3 catalysts with various compositions and prepared in various ways were investigated with quantitative ^{31}P and ^{27}Al solid state NMR. Samples without Co or Ni and samples containing magnesium instead of the paramagnetic element were included for comparison. For the impregnation of phosphorus, solutions of $NH_4H_2PO_4$ were used instead of H_3PO_4 solutions. It has been shown that, upon impregnation of phosphoric acid, partial solubilization of the Al^{3+} ion occurs and $AlPO_4$ is precipitated during the drying procedure (10). $NH_4H_2PO_4$ solutions are less acidic and the interaction with surface atoms of γ-Al_2O_3 is weaker. Other authors used $NH_4H_2PO_4$ solutions as well (17). Conclusions about the distribution of phosphates on our samples are therefore not directly transferable to H_3PO_4-impregnated γ-Al_2O_3. In addition, it should be mentioned that commercial catalysts are usually prepared by coimpregnation at low pH where the

0021-9517/97 $25.00

formation of heteropoly compounds plays an important role. In the present study the impregnation procedure was varied in order to be able to discriminate between various effects.

EXPERIMENTAL

Sample Preparation

Samples were prepared by pore volume impregnation of γ-Al_2O_3 (Condea, surface area 232 m^2/g, pore volume 0.5 cm^3/g) with aqueous solutions containing appropriate amounts of $NH_4H_2PO_4$ (Fluka), $(NH_4)_6Mo_7O_{24}\cdot 4H_2O$ (Merck), $Ni(NO_3)_2\cdot 6H_2O$ (Fluka), $Co(NO_3)_2\cdot 6H_2O$ (Johnson Matthey), or $Mg(NO_3)_2\cdot 6H_2O$ (Merck). The solutions were used without further adjustment of the pH; unless mentioned otherwise, the pH was between 4 and 6. The solutions containing phosphate as well as a metal nitrate salt had a pH of about 2. Solutions used for coimpregnating phosphorus, molybdenum, and nickel or cobalt (but not magnesium) had to be acidified with HNO_3 to obtain clear solutions, giving a final pH between 1 and 3. For coimpregnation of nickel and molybdenum, the salts had to be added to a 25 wt% aqueous solution of ammonia and to be heated to 120°C before a clear blue solution was formed. This solution remained stable even after cooling down to room temperature and had a pH of 9.

The amounts of the salts used in the impregnation were chosen to give catalysts with constant loadings: 2 wt% P, 8 wt% Mo, and 3 wt% Ni or Co, or 1.3 wt% Mg. Sequential impregnation, coimpregnation, or partial coimpregnation was applied and the samples were dried after each impregnation step at 110°C for 12 h in air. They were investigated in the dried form as well as after calcination for 2 h at 400°C in air following the last drying step. The catalysts are denoted by the order of impregnation and square brackets indicate coimpregnation of two or more elements. The element impregnated first is indicated next to the support.

Model compounds $CoAl_2O_4$ (Johnson Matthey), $Co_3(PO_4)_2\cdot 8H_2O$ (Johnson Matthey), and $MgHPO_4\cdot 3H_2O$ (Aldrich) were commercially available. $NiAl_2O_4$ and $MgAl_2O_4$ were prepared by mixing finely powdered stoichiometric amounts of γ-Al_2O_3 and NiO (Johnson Matthey) or MgO (Siegfried) and calcining the mixtures in air at 1400°C for 12 or 91 h, respectively. $Ni_3(PO_4)_2\cdot 8H_2O$ was prepared according to the method described by Bassett and Bedwell (18).

NMR Measurements

Samples containing phosphorus were investigated after drying (uncalcined) and after calcination. ^{31}P MAS NMR measurements were performed at a resonance frequency of 161.98 MHz. Chemical shifts were referenced to 85% phosphoric acid using $NH_4H_2PO_4$ as the secondary reference (0.9 ppm). Rotors were spun at 10 kHz and 2 μs pulses (40° pulses) were applied to obtain ^{31}P MAS spectra with proton high power decoupling. At least 1024 scans were acquired for each spectrum with a recycle time of 5 s. For a quantitative comparison of the signals of different samples the center band and the spinning sidebands were integrated; the measured intensities were corrected for deadtime effects ($I = I_{\text{measured}}\cdot \exp[\tau\cdot\pi\cdot\Delta\nu_{1/2}]$, where τ is receiver dead time and $\Delta\nu_{1/2}$ is full width at half height). $NH_4H_2PO_4$ was used as intensity standard.

All samples were investigated by ^{27}Al MAS NMR as well at a resonance frequency of 104.26 MHz. Chemical shifts were referenced to a 0.1 M $Al(NO_3)_3$ solution using $(NH_4)Al(SO_4)_2\cdot 12H_2O$ as the secondary reference (−0.4 ppm). Rotors were spun at 10 kHz and with an irradiation power of 63 kHz 10° flip angles were applied to obtain ^{27}Al MAS spectra. At least 512 scans were acquired for each spectrum with a recycle time of 10 s.

RESULTS

^{31}P NMR of Dried Samples

The chemical shift (peak position) of dried samples varied from a value of −8.2 ppm in a sample containing only phosphorus to values between −10 and −16 ppm in most other samples (Fig. 1a). The accuracy of these values is ±1 ppm. The chemical shift does not show a correlation with the impregnation method (sequential or coimpregnation). This chemical shift points to an advanced formation of polyphosphates instead of monophosphates (10). In coimpregnated samples this polyphosphate formation is favored due to competition for surface adsorption sites, since in most samples the surface is not large enough to accommodate all elements in a monolayer. The applied amount of phosphate corresponds to about 40% of a P_2O_5 monolayer, whereas molybdenum would cover about 65% of the surface in a MoO_3 monolayer. If part of the surface becomes occupied by other elements, less surface area is available for phosphate. As a consequence, part of the phosphate can only adsorb on adsorbed phosphate, facilitating polyphosphate formation. Even in the sequentially impregnated samples in which phosphate was impregnated first, polyphosphate may be formed, because phosphate may desorb again from the surface during the second impregnation step (only drying and no calcination was applied between two successive impregnations).

It is not likely that the observed shift from −8 to values between −10 and −16 ppm reflects the formation of metal phosphates like $M_3(PO_4)_2\cdot 8H_2O$ (M = Co, Ni, Mg). The reference compound $MgHPO_4\cdot 3H_2O$ showed signals at −5.0 and −7.6 ppm. In the literature only values for various magnesium phosphates can be found, ranging from 4.6 to −7.6 ppm for monophosphates and with signals at −13.1

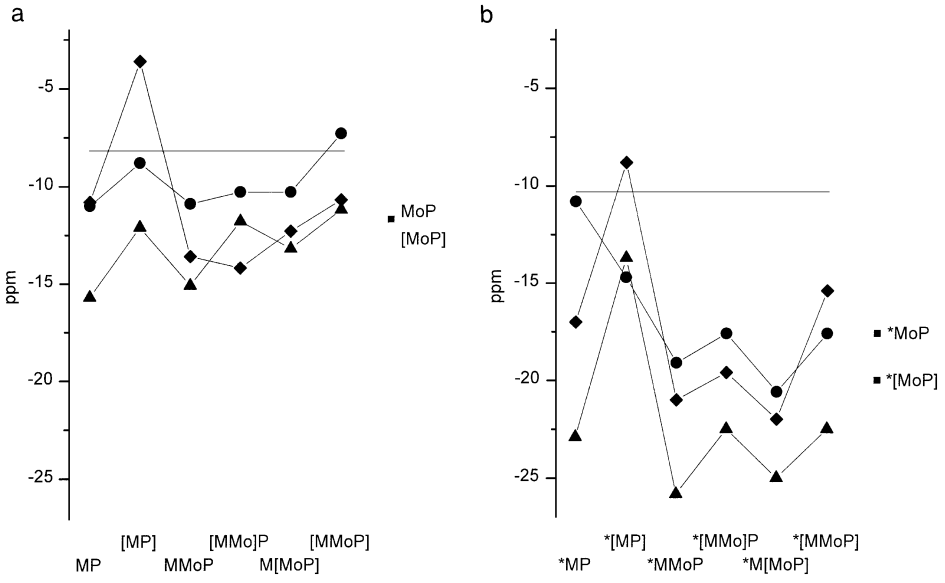

FIG. 1. Chemical shifts in ^{31}P MAS NMR spectra of (a) dried samples and (b) calcined samples; (◆) M = Co; (▲) M = Ni; (●) M = Mg; (—) P/γ-Al_2O_3; the results for samples without M are displayed at the right-hand side of each graph.

and −19.1 ppm for $Mg_2P_2O_7$, which contains two terminal phosphate groups in a diphosphate anion (19, 20). The type of phosphate (mono, di, or poly) seems to have a more profound influence on the chemical shift than the counter ion and it is, therefore, not possible to decide from the peak positions on the formation of metal phosphates. In addition, NMR signals of crystalline cobalt and nickel phosphates could not be obtained and on the magnesium-containing samples no signal with a linewidth as narrow as that of the $MgHPO_4 \cdot 3H_2O$ model compound was observed. Noteworthy is the rather high chemical shift of samples in which phosphorus and the metal were coimpregnated (mostly without molybdenum; −3.6 ppm for [CoP]/γ-Al_2O_3, −8.8 ppm for [MgP]/γ-Al_2O_3, −7.3 ppm for [MgMoP]/γ-Al_2O_3, and −12.1 ppm for [NiP]/γ-Al_2O_3) which cannot yet be explained.

The linewidth of the samples which do not contain paramagnetic cations (2600–2800 Hz) was smaller than that of samples containing cobalt (3700–4400 Hz) or nickel (2800–3600 Hz). This difference can be interpreted as a rough measure of an interaction of the phosphorus nuclei with the paramagnetic cobalt and nickel cations, the interaction with cobalt being stronger than that with nickel. No clear correlation was found between linewidth and impregnation method. The situation is slightly different when the distribution of the intensity over the center band and the spinning sidebands is considered. The intensity of the center band was lower in the samples with paramagnetic ions than in those without. The lowest center band intensities were always obtained when the paramagnetic metal salt was coimpregnated with the phosphate salt, especially when no molybdenum was present.

The overall intensity was more sensitive to the impregnation method employed than the chemical shifts and linewidths. For some samples the repeatability of the whole procedure of catalyst preparation and NMR measurement was checked; it showed that the measured intensities are accurate to about ±30% of the difference between the highest and lowest values of each series. The observed intensity differences of the ^{31}P NMR spectra will be discussed for the samples containing cobalt, since the trends are the same for the samples containing nickel, though less pronounced. First, the samples without molybdenum will be considered. The intensity of the sequentially impregnated CoP/γ-Al_2O_3 sample is only 14% of that of P/γ-Al_2O_3 or other samples without a paramagnetic element (see Fig. 2);

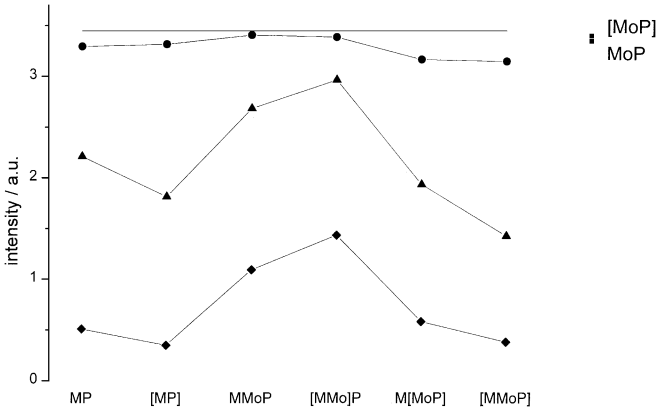

FIG. 2. Intensity of ^{31}P MAS NMR signals of dried samples; (◆) M = Co; (▲) M = Ni; (●) M = Mg; (—) P/γ-Al_2O_3; the results for samples without M are displayed at the right-hand side of the graph.

the intensity of the coimpregnated [CoP]/γ-Al_2O_3 sample is even lower (10%). In both cases, nothing hinders the paramagnetic cation from being close to phosphorus. The lower isoelectronic point of phosphate compared to the alumina surface even promotes the adsorption of Co ions on phosphate groups, and the ^{31}P NMR intensity can be maximally attenuated by the presence of the paramagnetic Co ions. When molybdenum is impregnated between phosphorus and cobalt, as in CoMoP/γ-Al_2O_3, the intensity is more than twice as high (31%), but still much less than in samples without cobalt. At least part of the phosphate must be shielded from the influence of cobalt by the molybdenum, either because a molybdate layer covers part of the phosphate groups or because compounds such as phosphomolybdate complexes were formed during the second impregnation step. It has been assumed that molybdate reacts preferentially with P–OH groups on a phosphated alumina surface (11, 17). Nonetheless, not all phosphate groups are covered by molybdate, since we know from proton NMR that some P–OH groups are still present, but fewer than in the sample without molybdenum (21). The formation of phosphomolybdate complexes has been observed only for a sample with a high molybdenum loading (12 wt%).

The ^{31}P NMR intensity rises to 41% of that of P/γ-Al_2O_3 when phosphorus is impregnated first and cobalt and molybdenum are impregnated together afterward ([CoMo]P/γ-Al_2O_3). Obviously, the cobalt then has less chance of coming into contact with the phosphorus. It is assumed that the preference of molybdenum for P–OH groups is higher than that of cobalt, since even without phosphorus, molybdate and nickel or cobalt ions adsorb on different sites of the alumina surface (22).

The phosphorus intensity is again rather low when molybdenum is coimpregnated together with phosphorus, either with or without cobalt. The intensity relative to that of P/γ-Al_2O_3 was 17% for Co[MoP]/γ-Al_2O_3 and 11% for [CoMoP]/γ-Al_2O_3. The signal to noise ratio in these spectra is so low that the uncertainty of these values is quite large. If phosphorus and molybdenum are coimpregnated (either with or without cobalt or nickel) phosphomolybdates (mainly $P_2Mo_5O_{26}^{6-}$ ions) form in the impregnation solution (23, 24). During adsorption on the alumina surface these complexes decompose due to preferential adsorption of the molybdate ions on basic sites and of the phosphate ions on more acidic sites (17, 25). Thus, the molybdate ions do not form a shielding layer on the phosphate groups. The cobalt or nickel cations are not hindered from reacting with the phosphate anions, resulting in a close interaction and a low ^{31}P NMR intensity.

Samples without a paramagnetic element, including those containing magnesium, have intensities which are about the same as that of P/γ-Al_2O_3. In this case no structural information can be obtained from the intensity values. The quantitative results described here are summarized in Fig. 2 and some spectra are shown in Fig. 3. At this stage the samples still contain counter ions (NH_4^+, NO_3^-), but the measurements do not give information on their whereabouts.

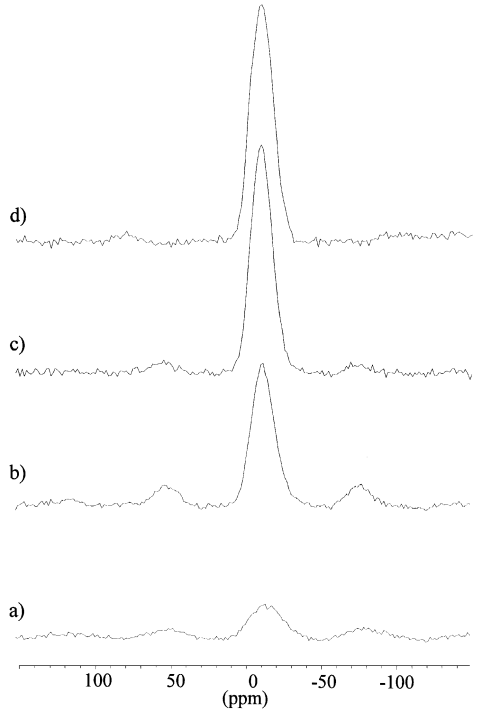

FIG. 3. Some ^{31}P MAS NMR spectra of dried samples: (a) [CoMo]P/γ-Al_2O_3; (b) [NiMo]P/γ-Al_2O_3; (c) [MgMo]P/γ-Al_2O_3; (d) P/γ-Al_2O_3.

^{31}P NMR of Calcined Samples

The samples described above were also measured after calcination at 400°C for 2 h. Compared to the dried samples the peak position generally shifted to lower frequencies (Fig. 1b). This shift was rather small for samples containing only phosphorus, the peak position being about −10.3 ppm. The shift can be explained either by aggregation of monophosphates to polyphosphates or by the formation of a second Al–O–P bond during the calcination step. Similar shifts also occurred for the other samples and were much more pronounced, with chemical shift values between −15.4 and −25.8 ppm. Values lower than −20 ppm indicate the formation of $AlPO_4$ (10, 14, 15, 26, 27) and most samples containing nickel were in this range. Two other trends were also observed. The more material deposited on the catalyst surface, the lower the chemical shift and the more $AlPO_4$ was formed. Second, sequential impregnation favored $AlPO_4$ formation. Some exceptions have to be mentioned. The three *[MP] samples on which cobalt, nickel, or magnesium was coimpregnated with phosphorus (but without molybdenum), as well as the *MgP sample sequentially impregnated with phosphorus and magnesium, had

markedly higher chemical shifts than the other samples of each series (−8.8, −13.7, −14.7, and −10.8 ppm). The shift of the cobalt sample was even higher than that of the sample containing only phosphorus. These samples showed a high chemical shift in the dried state as well.

The linewidth of most samples also increased after calcination. The samples containing nickel were an exception. Generally the greater linewidths indicate a greater variety of phosphorus compounds on the surface. Besides mono- and polyphosphates some aluminum phosphate and perhaps cobalt, nickel, or magnesium phosphates may have formed. The rather small linewidths of the nickel-containing samples is surprising. In addition, these lines are quite asymmetric. They are similar to the lineshape of amorphous $AlPO_4$ and have a chemical shift close to that of amorphous $AlPO_4$ (10, 14, 15, 26, 27). The formation of $AlPO_4$ would separate part of the phosphorus from the nickel, which would cause a smaller paramagnetic broadening. Seven other samples (*CoMoP/γ-Al_2O_3, *[CoMo]P/γ-Al_2O_3, *Co[MoP]/γ-Al_2O_3, *MgMoP/γ-Al_2O_3, *[MgMo]P/γ-Al_2O_3, *Mg[MoP]/γ-Al_2O_3, and *[MoP]/γ-Al_2O_3) also showed slight asymmetry. Six of these samples were loaded with three different elements and the second metal was not impregnated together with phosphorus. We conclude that these impregnation methods and the presence of nickel favor the formation of aluminum phosphate. In these calcined samples the distribution of the intensity over the center band and the spinning sidebands showed the same features as in the dried samples. The only difference was that the amount of intensity found in the center band of the calcined samples with cobalt or nickel is slightly higher than in the uncalcined samples, which proves that some separation of phosphorus and paramagnetic centers had occurred during calcination.

The same conclusion can be drawn from the fact that the overall intensity of calcined samples containing cobalt or nickel rose somewhat compared to dried samples (Figs. 4 and 5). Similar changes in intensity cannot be observed for samples without paramagnetic ions. Otherwise, the observations made for dried samples are also valid for the calcined samples. This rise in intensity upon calcination may partly be explained by the formation of aluminum phosphate. Another explanation may be a segregation of Co_3O_4 or NiO or the formation of cobalt or nickel molybdates (10). Such a segregation is in agreement with the surface areas of the calcined samples (Table 1). The surface area of samples containing Ni, Co, or Mg is generally similar or even higher than that of comparable samples without these elements, while the pore volume is lower. Pore plugging could explain a lower pore volume, but not a higher surface area. A higher surface area in combination with a lower pore volume points to the formation of small segregated particles on the carrier surface. Exceptions are the Co and Mg samples mentioned above containing aluminum phosphate, since the formation of $AlPO_4$ leads to pore plugging and correspondingly reduced surface areas.

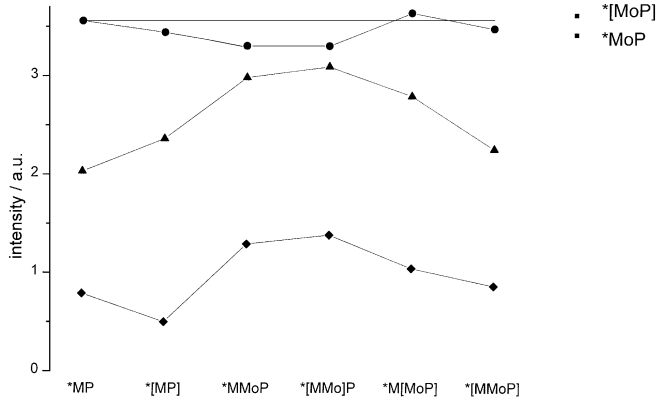

FIG. 4. Intensity of ^{31}P MAS NMR signals of calcined samples; (◆) M = Co; (▲) M = Ni; (●) M = Mg; (—) P/γ-Al_2O_3; the results for samples without M are displayed at the right-hand side of the graph.

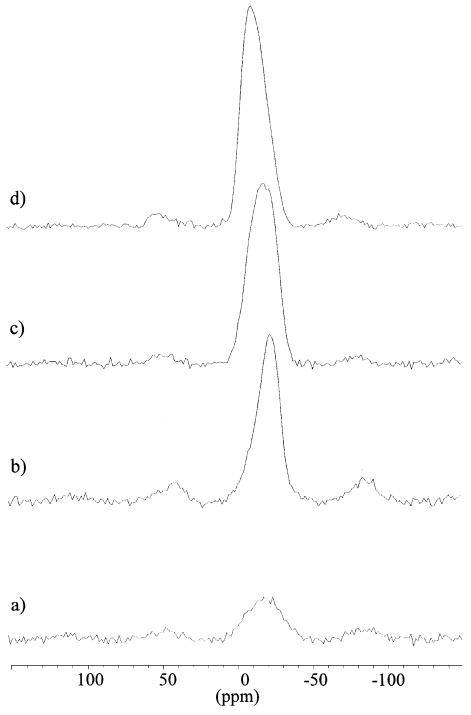

FIG. 5. Some ^{31}P MAS NMR spectra of calcined samples: (a) *[CoMo]P/γ-Al_2O_3; (b) *[NiMo]P/γ-Al_2O_3; (c) *[MgMo]P/γ-Al_2O_3; (d) *P/γ-Al_2O_3.

Since the ^{31}P NMR intensity of these samples was still quite low, it cannot be excluded that Co–Mo–P or Ni–Mo–P interaction phases were formed as well, as proposed in the literature (28, 29). It seems unlikely that some metal cations were incorporated into the Al_2O_3 spinel phase, since it was concluded from the easier reducibility of cobalt and nickel cations in TPR experiments that phosphorus inhibits the formation of $NiAl_2O_4$ or $CoAl_2O_4$, in which Ni

TABLE 1

Surface Areas and Pore Volumes of the Calcined Catalysts

Sample	Surface area (m^2/g)	Pore volume (cm^3/g)
γ-Al_2O_3	233	0.53
P/Al_2O_3	191	0.44
Mo/Al_2O_3	231	0.41
MoP/Al_2O_3	180	0.37
[MoP]/Al_2O_3	207	0.40
Ni/Al_2O_3	235	0.48
NiP/Al_2O_3	194	0.41
[NiP]/Al_2O_3	219	0.44
NiMo/Al_2O_3	225	0.41
[NiMo]/Al_2O_3[a]	220	0.40
NiMoP/Al_2O_3	181	0.36
Ni[MoP]/Al_2O_3	196	0.37
[NiMo]P/Al_2O_3[a]	186	0.36
[NiMoP]/Al_2O_3[b]	208	0.40
Co/Al_2O_3	230	0.48
CoP/Al_2O_3	200	0.42
[CoP]/Al_2O_3	215	0.45
CoMo/Al_2O_3	221	0.40
[CoMo]/Al_2O_3	217	0.41
CoMoP/Al_2O_3	177	0.36
Co[MoP]/Al_2O_3	193	0.37
[CoMo]P/Al_2O_3	175	0.36
[CoMoP]/Al_2O_3[b]	205	0.40
Mg/Al_2O_3	237	0.49
MgP/Al_2O_3	202	0.43
[MgP]/Al_2O_3	215	0.44
MgMo/Al_2O_3	218	0.41
[MgMo]/Al_2O_3	216	0.41
MgMoP/Al_2O_3	167	0.35
Mg[MoP]/Al_2O_3	193	0.38
[MgMo]P/Al_2O_3	186	0.38
[MgMoP]/Al_2O_3	199	0.39

[a] Molybdate and Ni nitrate dissolved in 25% NH_4OH.
[b] Acidified with HNO_3.

or Co ions are difficult to reduce (29, 30). In most samples without molybdenum the formation of $AlPO_4$ could not be proven by the ^{31}P NMR data, with the exception of the NiP/γ-Al_2O_3 catalyst. In the coimpregnated *[MP]/γ-Al_2O_3 samples (M = Co, Mg, Ni), the formation of aluminum phosphate was hindered by the formation of metal phosphates or similar compounds as described above. Accordingly, the chemical shifts of these samples remained quite high, even after calcination. For the sequentially impregnated samples (*MP/γ-Al_2O_3, M = Co, Mg), this observation is in contrast to the literature (10, 13–15, 31). In the literature, however, H_3PO_4 was generally used and this reacts much more strongly with the γ-Al_2O_3 surface than does $NH_4H_2PO_4$. Moreover, higher calcination temperatures ($\geq$500°C) were applied than in this study (400°C). Nonetheless, these authors also observed the existence of Co–P interaction phases.

^{27}Al NMR of Dried and Calcined Samples

O'Reilly (32) and Huggins and Ellis (33) showed that not all aluminum atoms of γ-Al_2O_3 can be detected by ^{27}Al NMR, most likely because they are in a highly distorted coordination at the alumina surface leading to large quadrupolar coupling constants. The aluminum atoms which remain detectable after adsorption of compounds on the surface do not seem to be affected very much by this adsorption because no change of the apparent shift (due to chemical shift and quadrupole interactions) was observed. The measured shifts were 7.1 ppm for octahedrally coordinated atoms (Al_o) and 65.2 ppm for tetrahedrally coordinated atoms (Al_t). In a sample containing only cobalt the peak positions seemed to be shifted to 2.1 and 60.5 ppm, but this could be due to line broadening. The ^{27}Al NMR signals of γ-Al_2O_3 were asymmetric, while the broadened lines of the Co/γ-Al_2O_3 samples were more symmetric, which may explain these shifts.

The linewidths again gave an indication of the presence and strength of paramagnetic interactions. They were largest in samples containing cobalt and smallest in samples with no paramagnetic ions. It is difficult to find a correlation between the linewidth and the impregnation method. The broadening seemed to be lowest when molybdenum was impregnated separately from the paramagnetic element.

Cobalt, nickel, and magnesium aluminate (spinel-type structures) were also measured. In cobalt aluminate the signal had vanished completely, while the signal of nickel aluminate amounted to only 2% of the alumina signal. The linewidths of the signals of $NiAl_2O_4$ and $MgAl_2O_4$ were significantly smaller than that of alumina. Therefore, formation of an appreciable amount of such a spinel, several layers thick, should be observable by a shoulder on the alumina signals, at least on the samples containing magnesium; this was not the case.

Some ^{27}Al NMR spectra of calcined samples are shown in Fig. 6. For the phosphorus-containing samples, the ^{27}Al NMR results supported the conclusions obtained from ^{31}P NMR. In those cases where ^{31}P NMR revealed the formation of $AlPO_4$, this was confirmed from line broadening of the tetrahedral line in the ^{27}Al NMR spectra in the 40 ppm region (compare Figs. 6b and 6c). This line broadening was stronger for nickel than for cobalt or magnesium containing samples, and it was stronger for samples in which phosphorus and the paramagnetic element were impregnated separately than for coimpregnated samples. This is again in accordance with the ^{31}P NMR results. A low ^{31}P NMR intensity due to adsorption of nickel or cobalt on the phosphate coincides with no evidence for $AlPO_4$ formation. This indicates a close proximity of Co (or Ni) to P and can be explained by the formation of Co–Mo–P compounds which hinder $AlPO_4$ formation.

Though quantification of the ^{27}Al NMR spectra is in principle possible, we refrained from doing so. It is known

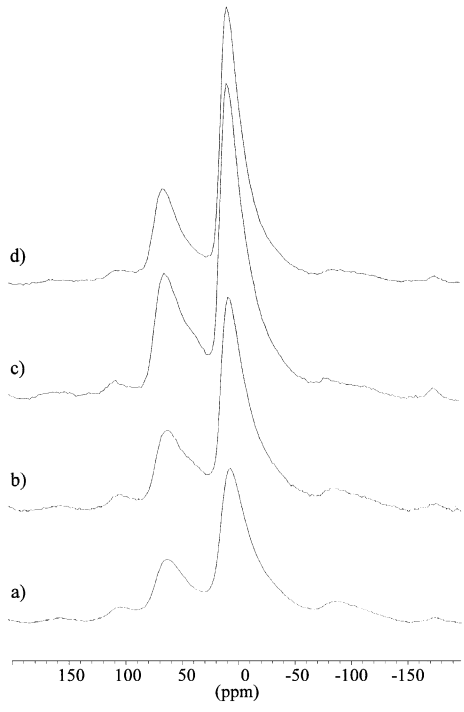

FIG. 6. Some ^{27}Al MAS NMR spectra of calcined samples: (a) *[CoMo]P/γ-Al_2O_3; (b) *[NiMo]P/γ-Al_2O_3; (c) *[MgMo]P/γ-Al_2O_3; (d) γ-Al_2O_3.

that the ^{27}Al MAS NMR intensity of γ-Al_2O_3 by itself is considerably lower than that of model compounds (32–34). This is due to a large quadrupolar broadening of signals from sites in distorted surroundings at the alumina surface. By exchange of the Al–OH protons by other ions (Mg, Ni, Co) upon impregnation, the degree of distortion and thus the signal intensity may change, even in the presence of nonparamagnetic ions (34). Therefore, quadrupolar effects may increase as well as decrease the ^{27}Al intensity, while paramagnetic effects decrease it. As a consequence, it is not possible to unambiguously determine and interpret the influence of the paramagnetic ions.

DISCUSSION

The Influence of Paramagnetic Elements on ^{27}Al and ^{31}P NMR Spectra

The main differences between the spectra of catalysts with and without paramagnetic elements are line broadening and loss of signal intensity. The extent of these differences depends mainly on the element employed and on structural differences. These effects must be due to the proximity of the paramagnetic element to the NMR nucleus (35). Such proximity usually gives rise to two interactions, namely the Fermi contact or hyperfine coupling due to the interaction of the nuclei with unpaired electron spin density delocalized at the nuclei themselves and the dipolar interaction between nuclear and electronic magnetic moment (36). Whereas the Fermi contact term is isotropic, the anisotropy of the dipolar coupling may change the distribution of the intensity over the isotropic band and the spinning sidebands in MAS NMR spectra (37). Due to electron relaxation processes the spin density delocalization and the orientation of the electronic magnetic moment change randomly, thus inducing nuclear relaxation as well. A shorter relaxation time may explain the increased linewidth of the NMR signal and may result in a signal loss during the receiver dead time after the application of the high frequency pulse (deadtime $\tau = 10\ \mu$s). If the paramagnetic ion is close to the ^{31}P or ^{27}Al atom, a signal loss can be expected; for greater distances a broadening of the line will be observed. Magnetic dipole interactions may also broaden the NMR line beyond observability if the linewidth is greater than the band width of the spectrometer. Another effect of a paramagnetic electron on a NMR nucleus can be envisioned. The chemical shift of the NMR nucleus can be increased due to the electron-nuclear dipolar-plus-contact term (38). In ^{31}P NMR studies of vanadium–phosphorus–oxide catalysts such shifts have been observed (39–41). Signals were found between −500 and 4500 ppm with the spin-echo mapping method. Static as well as rotor synchronized MAS spin-echo experiments with our *[NiP]/γ-Al_2O_3, *[CoP]/γ-Al_2O_3, $Co_3(PO_4)_2 \cdot 8H_2O$, and Co(3)P(2)/γ-Al_2O_3 samples did not reveal a new signal in the range −5000 to 5000 ppm. Nevertheless, the intensity of the signals of CoP/γ-Al_2O_3 increased in the spin-echo experiment relative to that of P/γ-Al_2O_3 from 15 to 32%. The linewidths of both the isotropic MAS line and the overall signal did not change. We conclude that some of the intensity loss is due to deadtime effects which can be canceled by the spin-echo experiment, but that the greater part is caused by broadening of the line beyond observability. Similar effects were found by Peeters *et al.* (42) in ^{31}P NMR investigations of cobalt-substituted aluminum phosphates. To explain the observed losses, they estimated that at least the first and third coordination spheres of the phosphorus atoms (not counting the oxygen atoms, the second sphere consists of aluminum atoms) around a paramagnetic cobalt center had become NMR invisible. Our samples were much more heterogeneous. $AlPO_4$ phases were observed in calcined samples. If the whole $AlPO_4$ surface were covered by cobalt atoms, the $AlPO_4$ phase would have to be several layers thick in order to get a ^{31}P NMR signal. Since the phosphorus and cobalt loadings on our catalysts are lower than monolayer coverage, it is very possible that only part of the $AlPO_4$ surface is in contact with cobalt atoms and that phosphorus atoms in another part far enough away are still visible. In samples which also contain molybdenum, molybdenum trioxide may furthermore form a shielding layer between the aluminum phosphate and the cobalt atoms. In dried samples, mono- and polyphosphate groups were usually observed.

If they were visible they were either adsorbed on different patches of the alumina surface than the cobalt or nickel ions or they were shielded by a molybdate layer from the paramagnetic element.

Very recently the spin-echo mapping technique was applied to cobalt phosphate, cobalt-substituted, and cobalt-impregnated aluminum phosphates (43). In the case of cobalt phosphate and cobalt-substituted $AlPO_4$, additional signals in the range 0–10,000 ppm were observed which could not be detected by MAS or spin-echo techniques. They were assigned to phosphorus atoms with at least one Co in the first coordination sphere. It might be interesting to check whether the spin-echo mapping technique is able to detect the missing phosphorus signals in our samples as well.

The effect of nickel cations on the NMR spectra is not as strong as that of cobalt cations. The broadening of the NMR lines is weaker and the signal loss is only about one-third to two-thirds of that observed in catalysts containing cobalt. Therefore, it is estimated that only the first and probably the second spheres of phosphate anion complexes become NMR invisible. The weaker effect of nickel is in accordance with its lower magnetic moment in the $^3A_2$ ground state in an octahedral position, compared to the higher magnetic moment and faster electron spin relaxation of the $^4T_1$ ground state of Co^{2+} ions in an octahedral position.

The Effect of Phosphate on the Hydrotreating Activity

One of the main effects of phosphorus incorporation into hydrotreating catalysts observed in this study was the formation of aluminum phosphate. This aluminum phosphate formed on the catalyst in its oxidic state has an influence on the sulfidation properties of the catalyst and on its catalytic activity (11, 12). An aluminum phosphate layer on γ-Al_2O_3 by itself is not sulfided below 1000°C. Cobalt and nickel compounds in contact with an $AlPO_4$ layer are less easily sulfided than when in contact with Al_2O_3 (12), in contrast to molybdate which is more easily sulfidable on samples containing phosphate (11). As a consequence the formation of Co_9S_8 or Ni_3S_2 is impeded and the probability of edge decoration of MoS_2 platelets by Co or Ni increases. This gives rise to the Co–Mo–S or Ni–Mo–S structure which is said to be the catalytically active phase for hydrodesulfurization and hydrodenitrogenation (44).

In this study, it was observed that aluminum phosphate formation is easier on catalysts containing nickel, whereas on samples that contain cobalt the formation of Co–Mo–P compounds seems to be more likely. Jian *et al.* have observed that the rate-determining step in the HDN of aniline, the hydrogenation to cyclohexylamine, is strongly promoted by the presence of phosphate in a sulfided NiMo/Al_2O_3 catalyst (45). Since the activation energy as well as the aniline adsorption energy were not affected, they concluded that the addition of phosphorus has a geometric effect, such as the increase of the number of MoS_2 stacks as observed by Ryan *et al.* (46). Large nitrogen-containing compounds can better coordinate to the active sites at the top of the MoS_2 stacks than to sites close to the Al_2O_3 surface. Since the occurrence of $AlPO_4$ increases the amount of molybdenum fractions in easily sulfidable forms, such as multilayered molybdate or MoO_3 (9), this should in turn lead to multilayered MoS_2 crystallites as well. When H_3PO_4 is used during catalyst preparation, $AlPO_4$ is formed by partial solubilization of Al cations and will occur to a greater extent than with $NH_4H_2PO_4$.

CONCLUSIONS

The existence of paramagnetic elements such as cobalt or nickel is an obstacle to NMR investigations of hydrotreating catalysts, because magnetic dipole interactions and decreased relaxation times lead to increased linewidths and signal losses. Cobalt has a stronger effect than nickel because of its higher magnetic moment and faster electron spin relaxation. Nonetheless, useful information about the effect of phosphorus and of impregnation procedures could be obtained by making use of the paramagnetic effects. It was observed that the formation of an amorphous $AlPO_4$ phase proceeds to a greater degree in the presence of nickel than in the presence of cobalt or magnesium, whereas the creation of Co–Mo–P interaction compounds is favored on cobalt-containing samples. An impregnation procedure in which phosphorus and the paramagnetic element are impregnated separately promotes $AlPO_4$ formation which is supposed to increase the stacking of MoS_2 and thus the HDN activity, whereas coimpregnation gives rise to a higher amount of Ni(Co)–Mo–P interaction compounds.

REFERENCES

1. Fitz, C. W., Jr., and Rase, H. F., *Ind. Eng. Chem. Prod. Res. Dev.* **22**, 40 (1983).
2. Tischer, R. E., Narain, N. K., Stiegel, G. J., and Cillo, D. L., *Ind. Eng. Chem. Res.* **26**, 422 (1987).
3. Eijsbouts, S., van Gestel, J. N. M., van Veen, J. A. R., de Beer, V. H. J., and Prins, R., *J. Catal.* **131**, 412 (1991).
4. Lewis, J. M., Kydd, R. A., Boorman, P. M., and van Rhyn, P. H., *Appl. Catal.* **84**, 103 (1992).
5. Mickelson, G. A., U.S. Patent 3,749,663, 1973.
6. Caceres, C. V., Fierro, J. L. G., Blanco, M. N., and Thomas, H. J., *Appl. Catal.* **10**, 333 (1984).
7. Atanasova, P., Halachev, T., Uchytil, J., and Kraus, M., *Appl. Catal.* **38**, 235 (1988).
8. Chadwick, D., Aitchison, D. W., Badilla-Ohlbaum, R., and Josefsson, L., *Stud. Surf. Sci. Catal.* **16**, 323 (1988).
9. López Cordero, R., López Guerra, L., Fierro, J. L. G., and López Agudo, A., *J. Catal.* **126**, 8 (1990).
10. DeCanio, E. C., Edwards, J. C., Scalzo, T. R., Storm, D. A., and Bruno, J. W., *J. Catal.* **132**, 498 (1991).
11. Lewis, J. M., and Kydd, R. A., *J. Catal.* **136**, 478 (1992).
12. Mangnus, P. J., van Langeveld, A. D., de Beer, V. H. J., and Moulijn, J. A., *Appl. Catal.* **68**, 161 (1991).

13. McMillan, M., Brinen, J. S., and Haller, G. L., *J. Catal.* **97**, 243 (1986).
14. Han, O. H., Lin, C. Y., and Haller, G. L., *Catal. Lett.* **14**, 1 (1992).
15. Han, O. H., Lin, C. Y., Sustach, N., McMillan, M., Carruther, J. D., Zilm, K. W., and Haller, G. L., *Appl. Catal. A* **98**, 195 (1993).
16. Edwards, J. C., and Ellis, P. D., *Langmuir* **7**, 2117 (1991).
17. van Veen, J. A. R., Hendriks, P. A. J. M., Andréa, R. R., Romers, E. J. G. M., and Wilson, A. E., *J. Phys. Chem.* **94**, 5282 (1990).
18. Bassett, H., and Bedwell, W. L., *J. Chem. Soc.* 854, 871 (1933).
19. Turner, G. L., Smith, K. A., Kirkpatrick, R. J., and Oldfield, E., *J. Magn. Reson.* **70**, 408 (1986).
20. Mudrakovskii, I. L., Shmachkova, V. P., Kotsarenko, N. S., and Mastikhin, V. M., *J. Phys. Chem. Solids* **47**, 335 (1986).
21. Kraus, H., and Prins, R., *J. Catal.* **164**, 260 (1996).
22. Spanos, N., and Lycourghiotis, A., *J. Colloid Interface Sci.* **171**, 306 (1995).
23. Pettersson, L., Andersson, I., and Öhman, L.-O., *Inorg. Chem.* **25**, 4726 (1986).
24. van Veen, J. A. R., Sudmeijer, O., Emeis, C. A., and de Wit, H., *J. Chem. Soc. Dalton Trans.* 1825 (1986).
25. Cheng, W.-C., and Luthra, N. P., *J. Catal.* **109**, 163 (1988).
26. Cheung, T. T. P., Willcox, K. W., Mc Daniel, M. P., and Johnson, M. M., *J. Catal.* **102**, 10 (1986).
27. van Eck, E. R. H., Kentgens, A. P. M., Kraus, H., and Prins, R., *J. Phys. Chem.* **99**, 16080 (1995).
28. Atanasova, P., and Halachev, T., *Appl. Catal.* **48**, 295 (1989).
29. Mangnus, P. J., van Veen, J. A. R., Eijsbouts, S., de Beer, V. H. J., and Moulijn, J. A., *Appl. Catal.* **61**, 99 (1990).
30. Atanasova, P., and López Agudo, A., *Appl. Catal. B* **5**, 329 (1995).
31. Gishti, K., Iannibello, A., Marengo, S., Morelli, G., and Titarelli, P., *Appl. Catal.* **12**, 381 (1984).
32. O'Reilly, D. E., *Adv. Catal.* **12**, 31 (1960).
33. Huggins, B. A., and Ellis, P. D., *J. Am. Chem. Soc.* **114**, 2098 (1992).
34. Kraus, H., Prins, R., and Kentgens, A. P. M., *J. Phys. Chem.* **100**, 16336 (1996).
35. Blumberg, W. E., *Phys. Rev.* **119**, 79 (1960).
36. La Mar, G. N., Horrocks, W. D., Jr., and Holm, R. H., "NMR of Paramagnetic Molecules," Chapter 1. Academic Press, New York, 1973.
37. Nayeem, A., and Yesinowski, J. P., *J. Chem. Phys.* **89**, 4600 (1988).
38. Abragam, A., "The Principles of Nuclear Magnetism," Chapter VI, Section II.C. Clarendon Press, Oxford, 1961.
39. Li, J., Lashier, M. E., Schrader, G. L., and Gerstein, B. C., *Appl. Catal.* **73**, 83 (1991).
40. Sananes, M. T., Tuel, A., Hutchings, G. J., and Volta, J. S., *J. Catal.* **148**, 395 (1994).
41. Sananes, M. T., and Tuel, A., *J. Chem. Soc. Chem. Commun.* 1323 (1995).
42. Peeters, M. P. J., van de Ven, L. J. M., de Haan, J. W., and van Hooff, J. H. C., *Colloids Surf. A* **72**, 87 (1993).
43. Canesson, L., and Tuel, A., *J. Chem. Soc. Chem. Commun.* 241 (1997).
44. Topsøe, H., Clausen, B. S., Candia, R., Wivel, C., and Mørup, S., *J. Catal.* **68**, 433 (1981).
45. Jian, M., Kapteijn, F., and Prins, R., *J. Catal.* **168**, 491 (1997).
46. Ryan, R. C., Kemp, R. A., Smegal, J. A., Denley, D. R., and Spinnler, G. E., *Stud. Surf. Sci. Catal.* **50**, 21 (1989).